Thermal Mechanisms of Millimeter Wave Stimulation of Excitable Cells

Mikhail G. Shapiro,[†‡§△*] Michael F. Priest,[¶||△] Peter H. Siegel,[†††‡‡] and Francisco Bezanilla[||*]
[†]Miller Research Institute, [‡]Department of Bioengineering, and [§]Department of Molecular and Cell Biology, University of California, Berkeley, CA; and [¶]Committee on Neurobiology and [||]Department of Biochemistry and Molecular Biology, University of Chicago, Chicago, IL; and [††]Jet Propulsion Laboratory and [‡‡]Department of Biology, California Institute of Technology, Pasadena, CA

ABSTRACT Interactions between millimeter waves (MMWs) and biological systems have received increasing attention due to the growing use of MMW radiation in technologies ranging from experimental medical devices to telecommunications and airport security. Studies have shown that MMW exposure alters cellular function, especially in neurons and muscles. However, the biophysical mechanisms underlying such effects are still poorly understood. Due to the high aqueous absorbance of MMW, thermal mechanisms are likely. However, nonthermal mechanisms based on resonance effects have also been postulated. We studied MMW stimulation in a simplified preparation comprising *Xenopus laevis* oocytes expressing proteins that underlie membrane excitability. Using electrophysiological recordings simultaneously with 60 GHz stimulation, we observed changes in the kinetics and activity levels of voltage-gated potassium and sodium channels and a sodium-potassium pump that are consistent with a thermal mechanism. Furthermore, we showed that MMW stimulation significantly increased the action potential firing rate in oocytes coexpressing voltage-gated sodium and potassium channels, as predicted by thermal terms in the Hodgkin-Huxley model of neurons. Our results suggest that MMW stimulation produces significant thermally mediated effects on excitable cells via basic thermodynamic mechanisms that must be taken into account in the study and use of MMW radiation in biological systems.

INTRODUCTION

Millimeter waves (MMWs), covering electromagnetic frequencies from 30 to 300 GHz, are finding increasing use in everyday technologies ranging from wireless telecommunications (1) to airport security scanners (2), automotive collision avoidance systems (3), and even nonlethal crowd control weaponry (4). Frequencies near 60 GHz are likely to become particularly ubiquitous due to their projected use in local area networks (5). In addition, MMWs have been investigated as a therapeutic modality in medical devices (6,7). Given their increasing utilization, there is considerable interest in the potential effects of MMWs on biological systems. In particular, a number of studies have documented the effects of MMWs on neural signaling. For example, prolonged MMW exposure was found to alter conditioned fear reflexes and pyramidal neuron spine density in rats (8), and produced a variety of electrophysiological effects in snail neurons (9), frog nerves (10), crayfish neurons (11), mouse nerves (12), and mouse cortical slices (13).

Despite these numerous observations, the underlying mechanisms by which MMWs alter neural activity are still unclear. Due to the high absorbance of MMWs by water (extinction coefficient $\approx$ 182 cm^{-1} at 60 GHz (14)), thermal mechanisms are considered likely (10,11). However, a number of investigators have interpreted the observed effects as requiring more complex explanations (9,12,13), such as hypothesized resonant interactions with membrane proteins and other cellular constituents. Unfortunately, because most studies of MMWs have been performed in relatively complex preparations such as innervated neuronal cultures, intact nerves, ganglia, and tissue slices, direct testing of molecular mechanisms has been challenging.

Here, we used a simplified preparation to directly examine the effects of MMWs on the function of key proteins involved in neuronal excitability. By expressing voltage-gated sodium and potassium channels and the sodium-potassium pump in *Xenopus laevis* oocytes, we were able to measure changes in activation and kinetic parameters induced by 60 GHz irradiation and compare them with the predicted effects of MMW-induced heating of the preparation. In addition, we studied how MMW-elicited changes in the activity of these molecules affected action potential (AP) firing. Our results provide support for the notion that a predominantly thermal mechanism underlies MMW stimulation.

MATERIALS AND METHODS

Membrane protein expression in oocytes

Xenopus laevis oocytes were surgically harvested and injected 1–2 days later with complementary RNA (cRNA) encoding the *Drosophila* voltage-gated potassium channel Shaker with fast inactivation removed (Δ6-46; 10 ng) (15), the α and β1 subunits of the rat $Na_v1.4$ (5 ng and 1 ng, respectively), the α and β subunits of the squid *Loligo pealeii* sodium-potassium pump (50 ng and 16.7 ng, respectively) (16), or a combination of Shaker (2.5 ng) and $Na_v1.4$ α and β1 (5 ng and 1 ng, respectively). cRNAs were transcribed using the mMESSAGE mMACHINE T7 kit (Life Technologies, Carlsbad, CA) using DNA from the pBSTA plasmid and linearized with NotI (New England Biolabs, Ipswich, MA). Oocytes were kept at 16°C in SOS solution containing (in mM) 96 NaCl, 2 KCl,

Submitted March 21, 2013, and accepted for publication May 7, 2013.

△Mikhail G. Shapiro and Michael F. Priest contributed equally to this work.

*Correspondence: mikhail@caltech.edu or fbezanilla@peds.bsd.uchicago.edu

Editor: Brian Salzberg.

0006-3495/13/06/2622/7 $2.00

http://dx.doi.org/10.1016/j.bpj.2013.05.014

1 $MgCl_2$, 1.8 $CaCl_2$, 10 HEPES, pH 7.4, supplemented with 50 mg/ml of gentamicin, until they were used in electrophysiology experiments.

Electrophysiology

Currents and voltages were measured 1–4 days after injection using an oocyte clamp (OC-725A; Warner Instruments, Hamden, CT) in a two electrode-voltage clamp configuration, operated by in-house software, at a room temperature of ~21°C. Sodium currents were measured in a bath solution containing (in mM) 28.75 NaOH, 90 N-methyl-D-glucamine-methanesulfonic acid (NMG-MES), 2 $Ca(OH)_2$, and 10 HEPES, using pipettes with 3 M KCl. Potassium currents were measured in a bath solution containing (in mM) 4 KOH, 115 NMG, 2 $Ca(OH)_2$, and 10 HEPES, using pipettes with 3 M CsCl. Sodium-potassium pump currents were measured in a bath solution containing (in mM) 5 K-MES, 100 Na-glutamate, 5 $BaCl_2$, 2 $NiCl_2$, 2 $MgCl_2$, and 5 HEPES after sodium was preloaded for 30–60 min in a loading solution containing (in mM) 90 Na-sulfate, 2.5 Na-citrate, and 5 HEPES. Ouabain was added at 10 μM concentration to confirm that the recorded currents came from the pump, and pipettes were filled with 3 M CsCl. APs in excitable oocytes, or excitocytes, expressing a combination of sodium and potassium channels were measured using the 100 MΩ mode on the clamp, which serves as a current clamp by connecting a 100 MΩ resistor in series with the current electrode. Excitocytes were recorded in a bath solution of SOS with 0.6 mM additional Ca^{2+} to facilitate AP firing, using pipettes with 3 M CsCl. To elicit AP trains, the holding current was adjusted for each oocyte so that the resting voltage would be between −100 mV and −85 mV. A 200 ms current pulse was then applied with its magnitude adjusted so as to elicit a train of six to eight spikes. The magnitude of the hyperpolarizing current varied between 100 and 250 nA among all oocytes, whereas the magnitude of the depolarizing current that elicited the AP train varied between ~200 and 400 nA among oocytes. These settings remained fixed across all the MMW powers or bath heating conditions tested for a given oocyte. For all experiments, the solutions were set to a pH of 7.4–7.5 and pipettes had a resistance of 0.2–2 MΩ.

MMW exposure

Continuous-wave (CW) and/or pulsed 60 GHz MMW power was produced using an Agilent E8257D signal generator (Agilent Technologies, Santa Clara, CA) operating at 15 GHz followed by an AMC15 frequency quadrupler (Millitech, Deerfield Park, MA) and an AMP-15, 60 GHz power amplifier (Fig. S1 in the Supporting Material). The maximum CW output power at the end of the waveguide port (see Fig. 1 *A*) was ~128 mW as measured with a calibrated thermistor sensor (ML83A; Anritsu America, Morgan Hill, CA). The 60 GHz radiofrequency (RF) power was delivered to the oocyte through an open-ended WR15 (3.81 × 1.905 mm aperture) rectangular, single-mode waveguide terminating ~1 mm below the bottom of the recording chamber. The chamber bottom was milled through and sealed over with a 0.25-mm-thick quartz coverslip on which the oocyte sat. Buffer solution filled the chamber to a depth of ~1.5 mm, completely covering the oocyte. The radiated RF power exiting the waveguide passed through the quartz, irradiated the bottom of the oocyte, and spread out to the surrounding buffer. After passing through the oocyte, the power was fully absorbed in the buffer before it reached the top of the solution. Because it was not possible to measure the RF power level directly, power density (mW/mm^2) at various positions along the optical path and in the surrounding fluid was inferred through electromagnetic simulations of the experimental setup using finite difference time domain (FDTD) software (Quickwave; QWED, Warsaw, Poland). Details of the simulation, including the parameters used, are provided in the Supporting Material. Sample plots from these FDTD simulations are shown in Fig. S2. Average power densities in the media at the bottom and top of the oocyte are reported in the Results section.

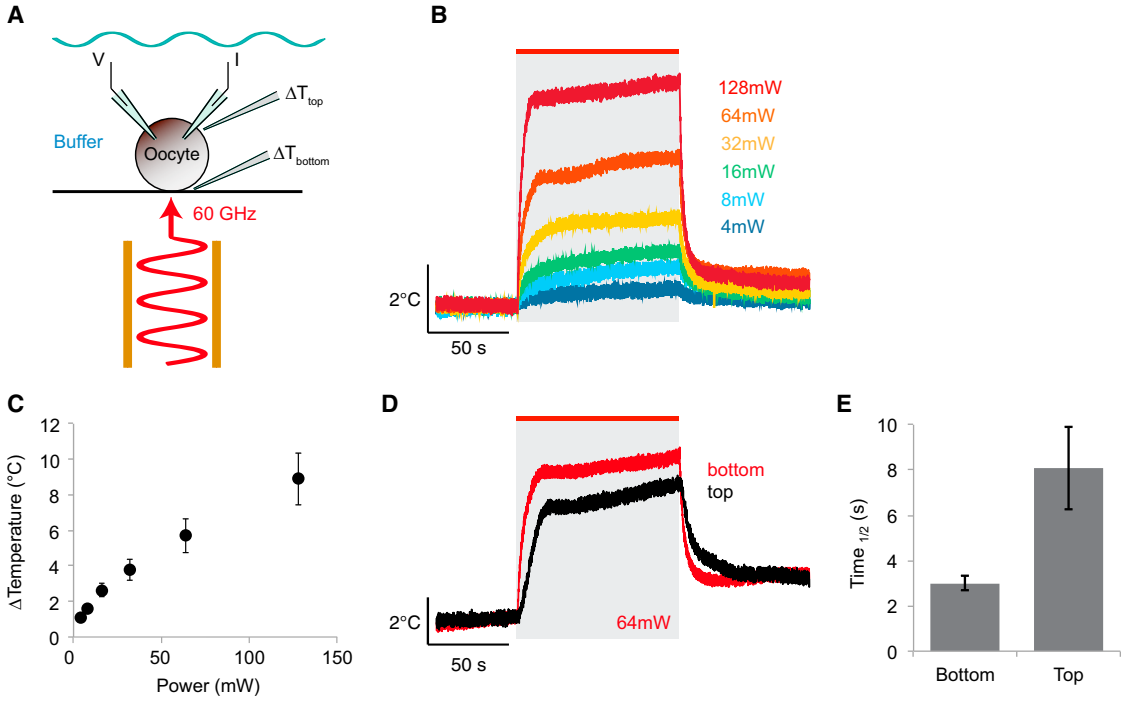

FIGURE 1 Temperature changes induced by MMW exposure. (*A*) Diagram of the experimental setup. A voltage-clamped oocyte rests on a quartz coverslip ~1 mm above a waveguide transmitting 60 GHz MMWs from an RF generator. Local changes in buffer temperature are measured via pipettes placed near the coverslip or above an oocyte. (*B*) Time course of temperature changes measured via pipette resistance at the bottom position in response to 100 s MMWs at varying power. (*C*) Maximal temperature change measured at each power ($N = 4$). (*D*) Time course of temperature change at the top and bottom positions in response to 64 mW MMWs. (*E*) Time to half-maximal temperature increase at the top and bottom positions after the start of 64 mW MMW stimulation ($N = 4$).

Before each exposure, the MMW power was set to a predetermined level using the ML83A via a waveguide switch. The signal level was set using a variable attenuator in the RF path (Fig. S1). During the exposures, the RF signal (CW or pulsed) was directly monitored with the use of a diode detector and directional coupler. By reading the detector voltage directly, we were able to record the actual RF pulse shape and relative amplitude incident on the oocyte, as set by the E8257D and after passage through the multiplier and power amplifier. Specimens were exposed to the MMWs for 100 s and given a 2-min rest period between MMW pulses. To study the time course of MMW effects on protein activity, we obtained electrophysiological recordings repetitively throughout this MMW pulse protocol. To study the effects of the MMWs on activity, we obtained electrophysiological recordings before the protocol, at the end of the MMW pulse sequence (which remained on during the measurement), and at the end of the rest period.

Bulk bath heating

For bulk heating experiments, a digital thermocouple (DP116 0.1°; Omega Engineering, Stamford, CT) was positioned in the bath solution within 1 mm of the oocyte to continuously record the bath temperature during electrophysiological recordings. The bath temperature was elevated by introducing a heated extracellular solution to the recording chamber, and allowed to cool over several minutes, during which time the excitocytes were stimulated to elicit AP trains as described above. AP trains occurring at specific temperatures above a 20°C baseline were automatically selected for analysis based on concurrent temperature recordings using MATLAB (The MathWorks, Natick, MA).

Data analysis and simulation

Data analysis was performed using an in-house analysis program and MATLAB. Kinetics were obtained by fitting exponential equations to sodium and potassium currents. The mean AP amplitude was determined as the mean difference between peak and immediately subsequent trough voltages. All error bars in plots represent the mean ± standard error (SE). Hodgkin-Huxley-based simulations of the nerve were performed in MATLAB using code adapted from the Membrane AP module of the Nerve program (available at http://nerve.bsd.uchicago.edu). The baseline temperature of the simulations was 6.3°C and was adjusted upward as indicated in the text.

Temperature measurements

Temperature increases resulting from MMW irradiation were made using pipet resistance, following the method of Yao et al. (17). Pipettes with a resistance of 5–10 MΩ were filled with solution matching the extracellular recording buffer containing (in mM) 120 NMG-MES, 20 HEPES, and 2 $Ca(OH)_2$, set to pH 7.4. The tip of the pipette was positioned in the bath above the center of the waveguide either as close as possible to the coverslip (approximating the position at the bottom of the oocyte) or just above an oocyte situated as described above. A 10 mV/MΩ current pulse was applied by the OC-725A amplifier to measure pipette resistance. A resistance-temperature calibration curve was obtained by applying hot solution (~45°C) to the bath and allowing it to cool while simultaneously recording pipette resistance and solution temperature. A linear calibration relationship was fit to the logarithm of resistance versus the inverse of absolute temperature. This calibrated relationship was used to convert resistance changes measured during the application of MMW pulses to temperature changes.

RESULTS

To study MMW effects, we constructed an experimental setup combining oocyte electrophysiology and local temperature measurements with 60 GHz stimulation applied in CW mode via a waveguide positioned just beneath the cell (Fig. 1 *A* and Fig. S1). We determined temperature changes elicited by MMW exposure using calibrated resistance measurements of pipette electrodes (17) positioned at the approximate locations of the bottom and top of the oocyte (Fig. 1, *A*, *B*, and *D*). We found that 100 s of MMW exposure produced maximal temperature elevations of 1.1°C ± 0.2°C to 8.9°C ± 1.5°C at output powers of 4–128 mW (corresponding to simulated power densities of 0.18–6 mW/mm^2 at the bottom of the oocyte and 0.01–0.33 mW/mm^2 at the top; Fig. 1 *C* and Fig. S2). The maximal increase in temperature at the top of the oocyte was approximately two-thirds of that observed at the bottom (Fig. 1 *D*). Because the oocyte is smaller than the opening of the waveguide, stimulation is expected to be uniform in the lateral plane, as confirmed by FDTD simulations of wave propagation (Fig. S2). At this power level, temperature increased with a $t_{1/2}$ of 3.0 ± 0.3 s at the bottom of the oocyte and 8.1 ± 1.8 s at its top (Fig. 1 *E*). This difference suggests that MMWs are efficiently absorbed by the bottommost region of buffer (consistent with Fig. S2), with more distal buffer regions heated primarily via thermal diffusion, reaching a steady state after 10–20 s of stimulation (Fig. 1, *B* and *D*). This is consistent with a characteristic thermal diffusion time in water of ~7 s over a 2 mm distance (given a thermal diffusivity of 0.143 mm^2 s^{-1}). At the powers used in this study, no major oocyte toxicity was observed after more than 2 h of stimulation, as evidenced by a lack of increased leakage current and unaltered electrophysiological responses.

To determine the effects of MMW irradiation on voltage-gated potassium channels, we recorded ionic currents in oocytes expressing the Shaker K_v channel using 60 ms depolarizing voltage steps from a holding potential of −70 mV before, during, and after MMW irradiation (in the "during" condition, MMWs were applied for 100 s before and during the pulse protocol). As shown in Fig. 2 *A* (for a step to −15 mV), MMWs reversibly accelerate channel activation. By repeating the pulse protocol during the application of MMWs, we observed that this change reached a plateau over a few seconds (Fig. 2 *B*) and its dynamics closely resembled those of MMW-induced heating (Fig. 1 *D*). The change in activation kinetics increased monotonically with MMW power (Fig. 2 *C*). In addition, MMW application slightly increased channel conductance (Fig. 2 *D*) and, again, higher power levels led to greater increases (Fig. 2 *E*).

The voltage-gated sodium channel $Na_v1.4$ (α with $\beta1$ subunit) also showed accelerated kinetics upon exposure to MMWs (Fig. 3, *A–C*). With 30 ms pulses from −100 mV to −15 mV, we observed a 1.33-fold acceleration of the inactivation rate with irradiation at 64 mW. The change in kinetics upon stimulation occurred over a timeframe similar to that observed for heating (Fig. 3 *B*), and the acceleration's magnitude increased monotonically with MMW power

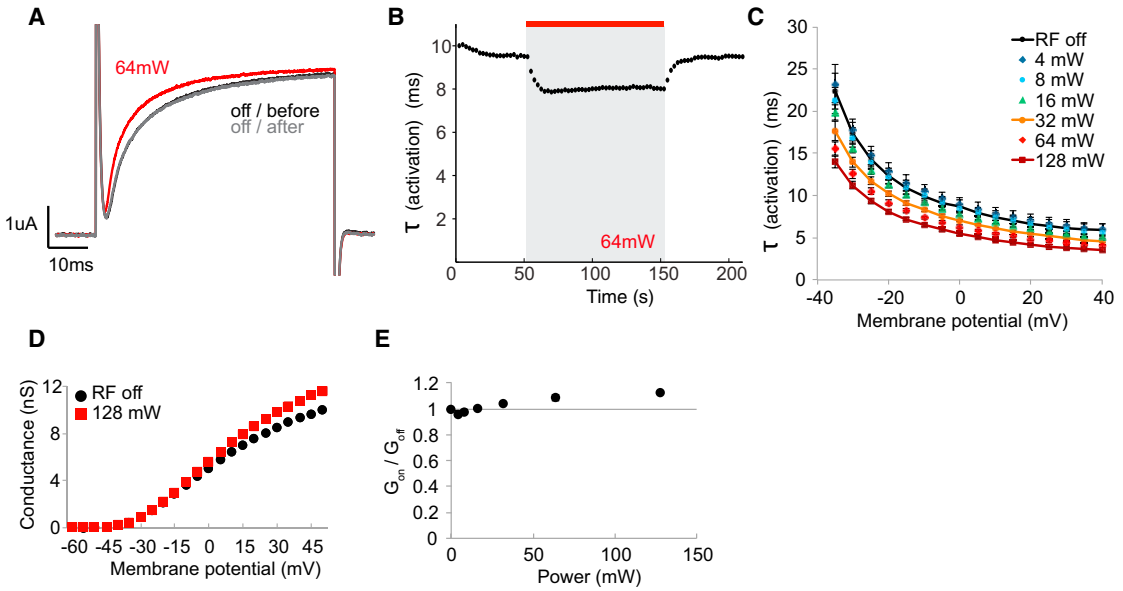

FIGURE 2 Effects of MMWs on the Shaker voltage-gated potassium channel. (*A*) Representative traces of a Shaker-injected oocyte's response to a depolarizing pulse from −70 mV to −15 mV before, during, and 100 s after a 64 mW MMW pulse. (*B*) Representative time course of activation time constant calculated from traces such as in *A* in response to 64 mW stimulation. (*C*) Activation time constant τ at different potentials with the application of various levels of MMW. Connecting lines are shown for three of the series as a visual aide. (*D*) Conductance-voltage response of a representative Shaker-injected oocyte with and without 128 mW MMWs. (*E*) Ratio of the conductances at 50 mV measured in individual cells with and without MMW application (G_{on}/G_{off}; $N = 4$). Error bars (mean ± SE) in *E* are smaller than the symbols.

(Fig. 3 *C*). Additionally, we observed a MMW-induced acceleration in the recovery from inactivation at −65 mV after a step pulse to −15 mV (Fig. 3 *D*, *inset*). The kinetics of this process varied with pulse power and were 2.33-fold faster with 64 mW MMW exposure than in the absence of stimulation (Fig. 3, *D* and *E*). Channel conductance showed

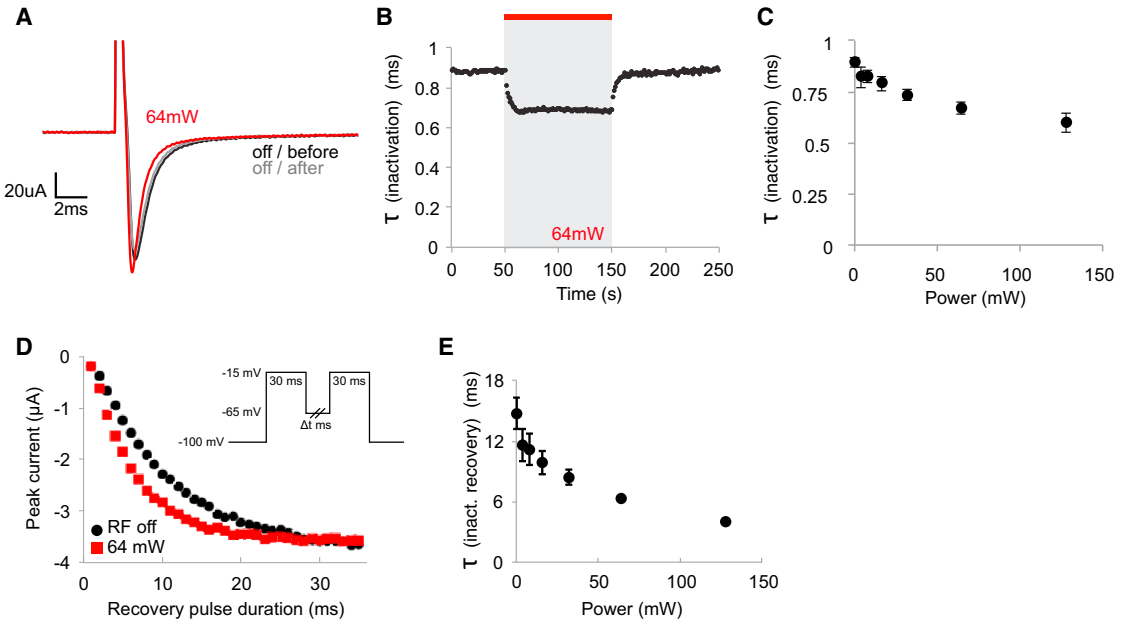

FIGURE 3 Effects of MMWs on the voltage-gated sodium channel $Na_V1.4$. (*A*) Representative traces of a $Na_V1.4$-injected oocyte to a voltage step from −100 mV to −15 mV before, during, and 100 s after a 64 mW MMW pulse. (*B*) Representative time course of the inactivation time constant calculated from traces such as in *A* in response to 64 mW stimulation. (*C*) Inactivation time constant for a step from −100 mV to −15 mV coincident with the application of various levels of MMWs ($N = 4$). (*D*) Recovery from inactivation as a function of recovery time (measured using the protocol shown in the *inset*) with and without MMW stimulation at 64 mW. (*E*) Inactivation recovery time constant obtained from experiments as in (*D*) at different MMW levels ($N = 4$).

a trend toward a slight increase upon MMW application, but the change was not statistically significant ($p > 0.1$; Fig. S3).

Although voltage-gated sodium and potassium channels are the main drivers of APs in neurons, the sodium-potassium pump is also essential for maintaining the requisite ionic gradients and membrane potential for spiking. Because the pump's activity has been implicated in MMW effects on neurons (9), we examined its response to MMW application in our system. Upon application of a 100 s MMW pulse (64 mW), pump current at a holding potential of 0 mV increased by 53% and then returned to baseline once the stimulation was turned off (Fig. 4, *A* and *B*). No change in holding current was observed when the pump was blocked with ouabain (Fig. 4 *A*). The dynamics of the increase in pump activity upon MMW irradiation were similar to those observed for the temperature and channel kinetics.

The observed accelerated kinetics of sodium and potassium channels in response to MMW stimulation would be expected to result in an increase in AP frequency in neurons responding to MMWs. To test this prediction, we used a simplified preparation in *Xenopus* oocytes that mimics the basic constituents of APs (18). After coinjecting oocytes with an appropriate ratio of voltage-gated sodium and potassium channels, we produced trains of APs by applying depolarizing current injections from a holding potential of ~−100 mV (Fig. 5 *A*). These excitable oocytes, or excitocytes, are a simple tool for dissecting the potential effects of external modulators on AP firing. As predicted, MMW exposure resulted in an increased spiking rate (Fig. 5 *A*). The interspike interval decreased monotonically with increasing MMW power (Fig. 5 *B*), becoming 35% shorter upon 64 mW stimulation. Again, the time course of change in the spiking interval upon the application of MMWs (Fig. 5 *C*) parallels that of the temperature change (Fig. 1, *B* and *D*). Furthermore, in separate experiments in which bulk heating was used to heat the bathing solution, temperature increases similar to those achieved with MMW exposure also resulted in similar accelerations in AP firing (Fig. 5, *D* and *E*). Additionally, both MMW and bulk heating led to small changes in the average AP amplitude (Fig. S4).

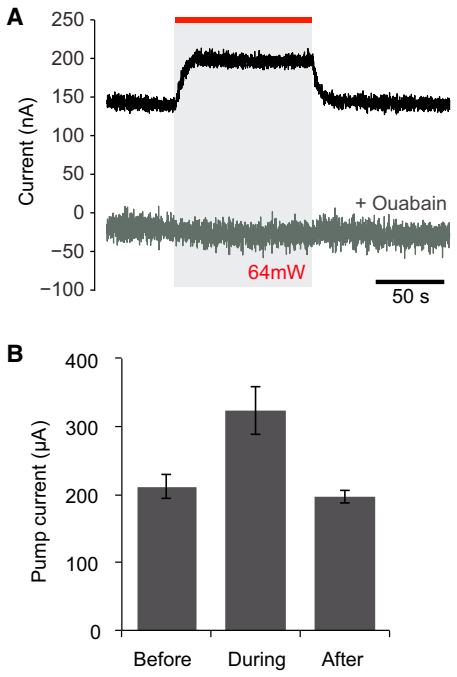

FIGURE 4 Effects of MMWs on the sodium-potassium pump. (*A*) Current recorded in a sodium-potassium pump-injected oocyte held at 0 mV, with a 100 s application of 64 mW MMWs, in the absence and presence of ouabain. (*B*) Pump-specific current (ouabain-sensitive) before, during, and 100 s after stimulation with 64 mW MMWs ($N = 5$).

DISCUSSION

Our results demonstrate a strong effect of MMW stimulation on the activity of three key proteins involved in neuronal excitability. In all cases, irradiation resulted in an acceleration of kinetics and/or an increase in activity. Furthermore, the combined effects on sodium and potassium channels resulted in a large increase in AP firing frequency in a model neuron. Simultaneously, MMW stimulation increased the temperature of our preparation by several degrees.

To determine whether the observed changes in channel and pump function could be explained by the observed heating, we first considered the direction and magnitude of the MMW effects. Directionally, our observations of accelerated kinetics (including in Shaker activation, $Na_v1.4$ inactivation, and $Na_v1.4$ recovery from inactivation) and the rate of sodium-potassium pump transport are consistent with heating, since increased temperature helps molecules surmount energy barriers in their reaction coordinates. By similar reasoning, increased channel conductance is also consistent with heating. Furthermore, changes in both kinetics and conductance increased with higher MMW power (and thus temperature). Quantitatively, we compared our experimental results with literature-reported Q_{10} values for each molecule (19–22). Based on observed fold changes in measured processes upon stimulation with 64 mW of MMW power (using 4.5°C temperature increase measured at the top of the oocyte), we calculated Q_{10} values in reasonably good agreement with the literature (Fig. 6 *A*). Importantly, we observed the expected relative thermal sensitivities of each process. For example, the nonstatistically significant increase observed in $Na_v1.4$ conductance likely arises from the low Q_{10} value of 1.49 previously reported for this process (19), whereas the large observed increase in sodium-pump activity likely arises from its high Q_{10} value of 4.3 (22).

Furthermore, MMW irradiation resulted in substantially shorter interspike intervals and somewhat smaller average

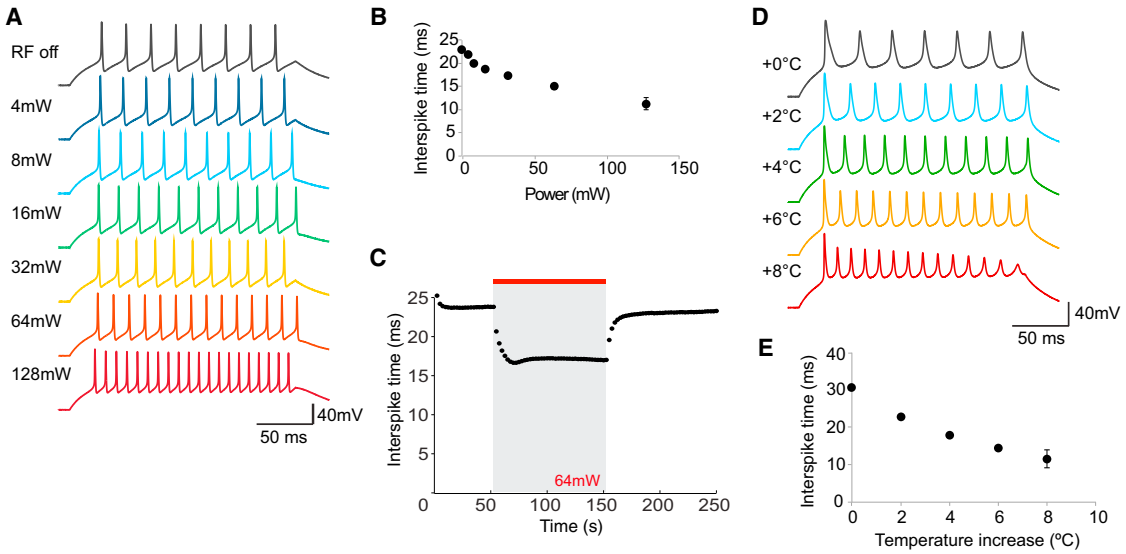

FIGURE 5 Effects of MMWs on AP firing. (*A*) Depolarization-stimulated AP trains in a representative excitocyte exposed to different levels of MMWs. (*B*) Interspike time as a function of MMW power ($N = 4$). (*C*) Representative time course of interspike time in response to 64 mW stimulation. (*D*) Depolarization-stimulated AP trains in a representative excitocyte exposed to different elevations of the bulk bath temperature. (*E*) Interspike time as a function of bulk bath temperature ($N = 5$). Where they are not visible, error bars are smaller than the plotted symbol.

AP amplitudes in our excitocyte preparation. These observations are qualitatively consistent with a nerve simulation based on Hodgkin-Huxley equations (23) in which the only parameter altered is the temperature (Fig. 6 *B*). We did not expect to find quantitative agreement, because the Q_{10} parameters used in the simulation do not precisely match those of the molecules used in our study. Interestingly, the model further predicts that increasing temperature past a certain point results in an abrogation of the AP train (Fig. S5). This effect was not observed reproducibly in our experiments at the MMW powers tested, but should be considered in other systems, which may have different exposure levels, relative channel and leak conductances, or Q_{10} parameters.

Second, we considered the time course of MMW-induced effects. If MMWs act on proteins through solution heating, then changes in their activity would be expected to follow the dynamics of the bath temperature (Fig. 1, *B* and *E*). If, on the other hand, MMWs interact with biomolecules directly, there is no reason to expect the resulting changes to accumulate over several seconds; in fact, one might expect the action of the MMWs to be immediate. In our study, changes in Shaker activation kinetics (Fig. 2 *B*), $Na_v1.4$ inactivation (Fig. 3 *B*), sodium-potassium pump current (Fig. 4 *A*), and AP interspike time (Fig. 5 *C*) all occurred with dynamics very similar to those observed for heating (Fig. 1, *B* and *D*).

Hence, in our simplified experimental system, the effects of MMWs are consistent with a straightforward mechanism based on solution heating. As MMW energy irradiates cells, it raises the temperature of the bath, resulting in acceleration of several key kinetic and actuation parameters. Remarkably, relatively modest changes in the kinetics of voltage-gated sodium and potassium channels lead to a profound increase in AP firing frequency. Although we cannot formally exclude them, we see no obvious nonthermal effects in our system. These findings are consistent with a prior report that the voltage-gated potassium channel in a mollusk neuron responds to MMWs in a manner that is wholly explainable by thermal effects (24).

Future studies are needed to deconstruct the thermal aspects of MMW response in more complex systems such as innervated cell cultures and intact organisms. Additionally, since the specific biomolecules responsible for neuronal excitability may have different Q_{10} values in different species, MMW responses may be species specific. Furthermore, the several-degree temperature changes transiently caused by irradiation may affect the function of other thermosensitive molecules in the cell, producing responses complementary to those characterized herein. Finally, it would be interesting to experiment with a broader range of electromagnetic frequencies, especially in the range of millimeters to a few microns, where other thermal mechanisms have been described (18,25).

SUPPORTING MATERIAL

Details of the FDTD simulations, supplementary figures, and references (26,27) are available at http://www.biophysj.org/biophysj/supplemental/S0006-3495(13)00570-5.

The authors thank John E. Carlstrom for the kind loan of the GHz signal generator, and Jorge E. Sanchez-Rodriguez for helpful discussions and reagents related to the sodium-potassium pump.

This research was supported by the Miller Research Institute (to MGS), NIH grant GM030376 (to FB) and F31 NIH-NS081954 (to MFP).

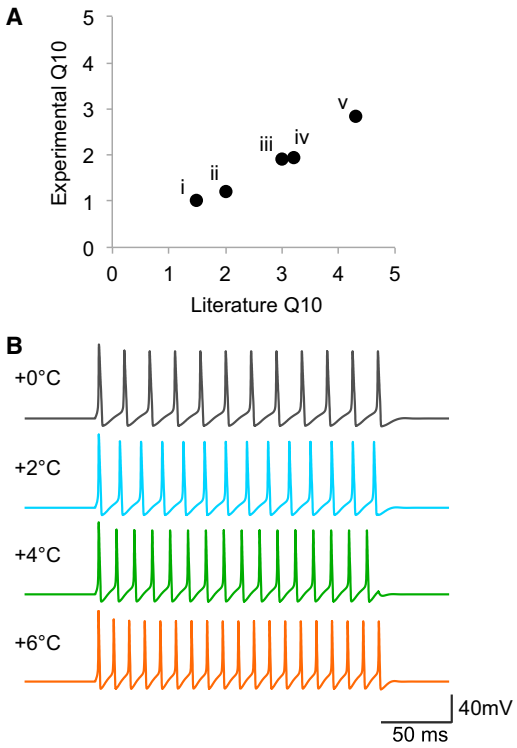

FIGURE 6 Comparison with theoretically predicted thermal effects. (*A*) Comparison of the Q_{10} values of $Na_V1.4$ conductance (i), Shaker conductance (ii), $Na_V1.4$ inactivation kinetics (iii), Shaker activation kinetics (iv), and sodium-potassium pump activity (v) reported in the literature with those calculated based on our experimental data, assuming a temperature increase of 4.5°C in response to a 100 s application of 64 mW MMWs. (*B*) AP traces generated by a computational implementation of the Hodgkin-Huxley model with system temperature increased by 0–6° from its baseline value.

All four authors planned the study, designed and performed experiments, and analyzed and interpreted the data. M.G.S. and M.F.P. wrote the manuscript with input from F.B. and P.H.S.

REFERENCES

1. Kallfass, I., J. Antes, …, A. Tessmann. 2011. All active MMIC-based wireless communication at 220 GHz. *IEEE Trans. Terahertz Sci. Technol.* 1:477–487.
2. Sheen, D. M., D. L. McMakin, and T. E. Hall. 2001. Three-dimensional millimeter-wave imaging for concealed weapon detection. *IEEE Trans. Microw. Theory.* 49:1581–1592.
3. Nicolson, S. T., K. H. Yau, …, S. P. Voinigescu, Sr. 2008. A low-voltage SiGe BiCMOS 77-GHz automotive radar chipset. *IEEE Trans. Microw. Theory.* 56:1092–1104.
4. Chen, Y., and M. Cui. 2012. Numerical study of deposition of energy of Active Denial Weapon in human skin. Asia-Pacific Symp. Electromagn. Compatibil., Singapore. 361–364.
5. IEEE Xplore. 2012. IEEE draft standard for local and metropolitan area networks. Specific requirements, part 11: Wireless LAN medium access control (MAC) and physical layer (PHY) specifications. Amendment 3: enhancements for very high throughput in the 60 GHz band. IEEE P802.11ad/D8.0. http://ieeexplore.ieee.org/xpl/mostRecentIssue.jsp?punumber=6212328. Accessed May, 2012.
6. Pakhomov, A. G., Y. Akyel, …, M. R. Murphy. 1998. Current state and implications of research on biological effects of millimeter waves: a review of the literature. *Bioelectromagnetics.* 19:393–413.
7. Siegel, P. H. 2004. Terahertz technology in biology and medicine. *IEEE Trans. Microw. Theory.* 52:2438–2447.
8. Gordon, Z. V., E. A. Lobanova, …, M. S. Tolgskaia. 1969. [Study of the biological effect of electromagnetic waves of millimeter range]. *Biull. Eksp. Biol. Med.* 68:37–39.
9. Alekseev, S. I., M. C. Ziskin, …, M. A. Bolshakov. 1997. Millimeter waves thermally alter the firing rate of the Lymnaea pacemaker neuron. *Bioelectromagnetics.* 18:89–98.
10. Pakhomov, A. G., H. K. Prol, …, C. B. Campbell. 1997. Search for frequency-specific effects of millimeter-wave radiation on isolated nerve function. *Bioelectromagnetics.* 18:324–334.
11. Khramov, R. N., E. A. Sosunov, …, V. V. Lednev. 1991. Millimeter-wave effects on electric activity of crayfish stretch receptors. *Bioelectromagnetics.* 12:203–214.
12. Alexseev, S. I., O. V. Gordiienko, …, M. C. Ziskin. 2010. Millimeter wave effects on electrical resopnses of the sural nerve in vivo. *Bioelectromagnetics.* 30:180–190.
13. Pikov, V., X. Arakaki, …, P. H. Siegel. 2010. Modulation of neuronal activity and plasma membrane properties with low-power millimeter waves in organotypic cortical slices. *J. Neural Eng.* 7:045003.
14. Querry, M. R., D. M. Wieliczka, and D. J. Segelstein. 1991. Water (H2O). *In* Handbook of Optical Constants of Solids II. E. D. Palik, editor.. Academic Press, Boston, MA. 1059–1077.
15. Hoshi, T., W. N. Zagotta, and R. W. Aldrich. 1990. Biophysical and molecular mechanisms of Shaker potassium channel inactivation. *Science.* 250:533–538.
16. Colina, C., J. J. Rosenthal, …, M. Holmgren. 2007. Structural basis of Na(+)/K(+)-ATPase adaptation to marine environments. *Nat. Struct. Mol. Biol.* 14:427–431.
17. Yao, J., B. Liu, and F. Qin. 2009. Rapid temperature jump by infrared diode laser irradiation for patch-clamp studies. *Biophys. J.* 96:3611–3619.
18. Shapiro, M. G., K. Homma, …, F. Bezanilla. 2012. Infrared light excites cells by changing their electrical capacitance. *Nat Commun.* 3:736.
19. Kirsch, G. E., and J. S. Sykes. 1987. Temperature dependence of Na currents in rabbit and frog muscle membranes. *J. Gen. Physiol.* 89:239–251.
20. Ruff, R. L. 1999. Effects of temperature on slow and fast inactivation of rat skeletal muscle Na+ channels. *Am. J. Physiol.* 277:C937–C947.
21. Iverson, L. E., M. A. Tanouye, …, B. Rudy. 1988. A-type potassium channels expressed from Shaker locus cDNA. *Proc. Natl. Acad. Sci. USA.* 85:5723–5727.
22. Castillo, J. P., D. De Giorgis, …, F. Bezanilla. 2011. Energy landscape of the reactions governing the Na+ deeply occluded state of the Na+/K+-ATPase in the giant axon of the Humboldt squid. *Proc. Natl. Acad. Sci. USA.* 108:20556–20561.
23. Hodgkin, A. L., and A. F. Huxley. 1952. A quantitative description of membrane current and its application to conduction and excitation in nerve. *J. Physiol.* 117:500–544.
24. Alekseev, S. I., and M. C. Ziskin. 1999. Effects of millimeter waves on ionic currents of Lymnaea neurons. *Bioelectromagnetics.* 20:24–33.
25. Wilmink, G. J., and J. E. Grundt. 2011. Invited review article: current state of research on biological effects of terahertz radiation. *J. Infrared. Milli. Terahz. Waves.* 32:1074–1122.
26. Bezanilla, F., E. Rojas, and R. E. Taylor. 1970. Sodium and potassium conductance changes during a membrane action potential. *J. Physiol.* 211:729–751.
27. Rosenthal, J. J., and F. Bezanilla. 2002. A comparison of propagated action potentials from tropical and temperate squid axons: different durations and conduction velocities correlate with ionic conductance levels. *J. Exp. Biol.* 205:1819–1830.